



HAL
open science

Staggered grid residual distribution scheme for Lagrangian hydrodynamics

Remi Abgrall, Tokareva Svetlana

► **To cite this version:**

Remi Abgrall, Tokareva Svetlana. Staggered grid residual distribution scheme for Lagrangian hydrodynamics: Staggered grid RD scheme for Lagrangian hydrodynamics. 2016. hal-01327473v1

HAL Id: hal-01327473

<https://inria.hal.science/hal-01327473v1>

Preprint submitted on 6 Jun 2016 (v1), last revised 2 May 2017 (v2)

HAL is a multi-disciplinary open access archive for the deposit and dissemination of scientific research documents, whether they are published or not. The documents may come from teaching and research institutions in France or abroad, or from public or private research centers.

L'archive ouverte pluridisciplinaire **HAL**, est destinée au dépôt et à la diffusion de documents scientifiques de niveau recherche, publiés ou non, émanant des établissements d'enseignement et de recherche français ou étrangers, des laboratoires publics ou privés.

1 **STAGGERED GRID RESIDUAL DISTRIBUTION SCHEME**
2 **FOR LAGRANGIAN HYDRODYNAMICS***

3 RÉMI ABGRALL[†] AND SVETLANA TOKAREVA[‡]

4 **Abstract.** This paper is focused on the Residual Distribution (RD) interpretation of the Do-
5 brev et al. scheme [Dobrev et al., SISC, 2012] for the numerical solution of the Euler equations
6 in Lagrangian form. The first ingredient of the original scheme is the staggered grid formulation
7 which uses continuous node-based finite element approximations for the kinematic variables and cell-
8 centered discontinuous finite elements for the thermodynamic parameters. The second ingredient of
9 the Dobrev et al. scheme is an artificial viscosity technique applied in order to make possible the
10 computation of strong discontinuities. The aim of this paper is to provide an efficient mass matrix
11 diagonalization method in order to avoid the inversion of the global sparse mass matrix while keep-
12 ing all the accuracy properties and to construct a parameter-free stabilization of the scheme to get
13 rid of the artificial viscosity. In addition, we study the conservation and entropy properties of the
14 constructed RD scheme. To demonstrate the robustness of the proposed RD scheme, we solve several
15 one-dimensional shock tube problems from rather mild to very strong ones.

16 **Key words.** Residual distribution scheme, Lagrangian hydrodynamics, finite elements

17 **AMS subject classifications.** 65M60, 76N15, 76L05

18 **1. Introduction.** We are interested in the numerical solution of the Euler equa-
19 tions in Lagrangian form. This problem has motivated many researchers, starting from
20 the seminal work of von Neumann and Richtmyer [28], to more recent works such as
21 [12, 20, 5, 22]. Most of these works deal with schemes that are formally second order
22 accurate. Up to our knowledge, there are much less works dealing with (formally)
23 high order methods: either they are of discontinuous Galerkin type [25, 26, 27], use a
24 staggered finite element formulation [15] or an ENO/WENO formalism [13], see also
25 the recent developments in [7, 17, 8, 16, 6, 10, 9].

26 In the discontinuous Galerkin (DG) formulation, all variables are described inside
27 elements, while in the staggered grid formulation, the approximations of the thermo-
28 dynamic parameters (such as pressure, specific internal energy or volume/density) are
29 cell-centered, and thus possibly discontinuous across elements as in the DG method,
30 while the velocity approximation is node-based, that is, it is described by a function
31 that is polynomial in each element and globally continuous in the whole computa-
32 tional domain. In a way this is a natural extension of the Wilkins' scheme [29] to
33 higher order of accuracy.

34 This paper is focused on Dobrev et al. [15] formulation. This formulation, that
35 we describe in more detail below, uses two ingredients. First, starting from the fi-
36 nite element formulation, one needs to introduce a global mass matrix that is block
37 diagonal on the thermodynamic parameters (as in DG method) but leads to a sparse
38 symmetric matrix for the velocity components (as in finite element method). Hence,
39 the treatment of the mass matrix consists of an inversion¹ of a block diagonal matrix,
40 which is cheap, but also of a sparse symmetric positive definite matrix, which is more
41 expensive both in terms of CPU time and memory. In addition, every time when
42 mesh refinement or remapping is needed (which is typical for Lagrangian methods),

*This work was funded by SNFS via the grant # 200021_153604

[†]Institute of Mathematics, University of Zurich, Switzerland (remi.abgrall@math.uzh.ch).

[‡]Institute of Mathematics, University of Zurich, Switzerland (svetlana.tokareva@math.uzh.ch).

¹By saying "inversion of a matrix" we mean the solution of a linear system with the corresponding matrix.

43 this global matrix needs to be recomputed. The second ingredient of the Dobrev et al.
 44 scheme is an artificial viscosity technique applied in order to make possible the com-
 45 putation of strong discontinuities. Note that the staggered formulation automatically
 46 guaranties linear stability.

47 The aim of this paper is to give answers to two questions: (i) can we avoid
 48 the inversion of the large sparse global mass matrix while keeping all the accuracy
 49 properties and (ii) can we construct a parameter-free artificial viscosity? In order
 50 to answer these questions, we rely on the Residual Distribution (RD) interpretation
 51 of the Dobrev et al. scheme and show how to modify it without introducing any
 52 additional complexity in the formulation.

53 The format of this contribution is as follows. We first give the formulation of the
 54 Euler equations in Lagrangian form and then recall Dobrev et al. formulation. Next,
 55 we introduce the RD formulation and show how to guarantee, when the scheme is
 56 stable, the convergence to a weak solution. Of course Dobrev et al. method satisfies
 57 these conditions, but the analysis presented in this paper opens new doors. Using the
 58 RD formulation, we show how to construct a simple first order scheme and how to
 59 increase the spatial accuracy. The next step is to explain the diagonalization of the
 60 global sparse mass matrix without the loss of accuracy: this is obtained by applying
 61 ideas coming from [21, 2]. We conclude by considering several one-dimensional shock
 62 tube problems from rather mild to very strong blast problems.

63 **2. Governing equations.** We consider a fluid domain $\Omega_0 \subset \mathbb{R}^d$, $d = 1, 2, 3$ that
 64 is deforming in time through the movement of the fluid. In what follows, \mathbf{X} denotes
 65 any point of Ω_0 , while \mathbf{x} denotes any point of Ω_t , the domain obtained from Ω_0 under
 66 deformation. We assume the existence of a one-to-one mapping Φ from Ω_0 to Ω_t such
 67 that $\mathbf{x} = \Phi(\mathbf{X}, t) \in \Omega_t$ for any $\mathbf{X} \in \Omega_0$. We will call \mathbf{X} the Lagrangian coordinates
 68 and \mathbf{x} the Eulerian ones. The Lagrangian description corresponds to the one of an
 69 observer moving with the fluid. In particular, its velocity, which coincides with the
 70 fluid velocity, is given by:

$$71 \quad (1a) \quad \mathbf{u}(\mathbf{x}, t) = \frac{d\mathbf{x}}{dt} = \frac{\partial \Phi}{\partial t}(\mathbf{X}, t).$$

72 We also introduce the deformation tensor \mathbb{J} (Jacobian matrix),

$$73 \quad (1b) \quad \mathbb{J}(\mathbf{x}, t) = \nabla_{\mathbf{X}} \Phi(\mathbf{X}, t) \text{ where } \mathbf{x} = \Phi(\mathbf{X}, t).$$

74 Hereafter, the notation $\nabla_{\mathbf{X}}$ corresponds to the differentiation with respect to La-
 75 grangian coordinates, while $\nabla_{\mathbf{x}}$ — to the Eulerian ones.

76 It is well known that the equations describing the evolution of fluid particles are
 77 consequences of the conservation of mass, momentum and energy, as well as a technical
 78 relation, the Reynolds transport theorem. It states that for any scalar quantity $\alpha(\mathbf{x}, t)$,
 79 we have:

$$80 \quad (1c) \quad \frac{d}{dt} \int_{\omega_t} \alpha(\mathbf{x}, t) d\mathbf{x} = \int_{\omega_t} \frac{\partial \alpha}{\partial t}(\mathbf{x}, t) d\mathbf{x} + \int_{\partial \omega_t} \alpha(\mathbf{x}, t) \mathbf{u} \cdot \mathbf{n} d\sigma = \int_{\omega_t} \left(\frac{d\alpha}{dt} + \mathbf{u} \cdot \nabla_{\mathbf{x}} \alpha \right) d\mathbf{x}$$

81 In this relation, the set ω_t is the image of any set $\omega_0 \subset \Omega_0$ by Φ , i.e. $\omega_t = \Phi(\omega_0, t)$,
 82 $d\sigma$ is the measure on the boundary of $\partial \omega_t$ and \mathbf{n} is the outward unit normal. The
 83 gradient operator is taken with respect to the Eulerian coordinates.

84 The conservation of mass reads: for any $\omega_0 \subset \Omega_0$,

$$85 \quad \frac{d}{dt} \int_{\omega_t} \rho d\mathbf{x} = 0, \quad \omega_t = \Phi(\omega_0, t),$$

86 so that we get, defining $J(\mathbf{x}, t) = \det \mathbb{J}(\mathbf{x}, t)$,

$$87 \quad (1d) \quad J(\mathbf{x}, t)\rho(\mathbf{x}, t) = \rho(\mathbf{X}, 0) := \rho_0(\mathbf{X}).$$

88 Using Reynolds' transport theorem (1c), we get that for any function f (real or
89 vectorial),

$$90 \quad (1e) \quad \frac{d}{dt} \int_{\omega_t} \rho f \, d\mathbf{x} = \int_{\omega_t} \rho \frac{df}{dt} \, d\mathbf{x}.$$

91 Newton's law states that the acceleration is equal to the sum of external forces,
92 so that

$$93 \quad \frac{d}{dt} \int_{\omega_t} \rho \mathbf{u} \, d\mathbf{x} = - \int_{\partial\omega_t} p \mathbf{n} \, d\sigma,$$

94 and thus, using (1c),

$$95 \quad (1f) \quad \rho \frac{d\mathbf{u}}{dt} + \nabla_{\mathbf{x}} p = 0.$$

96 The pressure $p(\mathbf{x}, t)$ is a thermodynamic characteristic of a fluid and in the simplest
97 case a function of two independent thermodynamic parameters, for example the spe-
98 cific energy ε and the density,

$$99 \quad (1g) \quad p = p(\rho, \varepsilon).$$

100 The total energy of a fluid particle is $\rho e = \rho\varepsilon + \frac{1}{2}\rho\mathbf{u}^2$. Using the first principle
101 of thermodynamics, the variation of energy is the sum of variations of heat and the
102 work of the external forces. Assuming an isolated system, we get

$$103 \quad \frac{d}{dt} \int_{\omega_t} \rho \left(\varepsilon + \frac{1}{2} \mathbf{u}^2 \right) \, d\mathbf{x} = - \int_{\partial\omega_t} p \mathbf{u} \cdot \mathbf{n} \, d\sigma,$$

104 i.e.

$$105 \quad (1h) \quad \rho \frac{d\varepsilon}{dt} + p \nabla_{\mathbf{x}} \cdot \mathbf{u} = 0.$$

106 **3. Staggered grid scheme of Dobrev et al.** Here we briefly recall the main
107 ideas of the staggered grid method proposed in [15]. The semi-discrete approximation
108 of (1) is sought for such that the velocity field \mathbf{u} belongs to a kinematic space $\mathcal{V} \subset$
109 $(H^1(\Omega_0))^d$ of finite dimension; it has a basis denoted by $\{w_{i_{\mathcal{V}}}\}_{i_{\mathcal{V}} \in \mathcal{D}_{\mathcal{V}}}$, the set $\mathcal{D}_{\mathcal{V}}$
110 is the set of kinematic degrees of freedom (DOFs) with the total number of DOFs
111 given by $\#\mathcal{D}_{\mathcal{V}} = N_{\mathcal{V}}$. The thermodynamic quantities such as the internal energy ε
112 are sought for in a thermodynamic space $\mathcal{E} \subset L^2(\Omega_0)$. As before, this space is finite
113 dimensional, and its basis is $\{\phi_{i_{\mathcal{E}}}\}_{i_{\mathcal{E}} \in \mathcal{D}_{\mathcal{E}}}$. The set $\mathcal{D}_{\mathcal{E}}$ is the set of thermodynamical
114 degrees of freedom with the total number of DOFs $\#\mathcal{D}_{\mathcal{E}} = N_{\mathcal{E}}$. In the following, the
115 subscript \mathcal{V} (resp. \mathcal{E}) refers to kinematic (resp. thermodynamic) degrees of freedom.

116 The fluid particle position \mathbf{x} is approximated by:

$$117 \quad (2a) \quad \mathbf{x} = \Phi(\mathbf{X}, t) = \sum_{i_{\mathcal{V}} \in \mathcal{D}_{\mathcal{V}}} \mathbf{x}_{i_{\mathcal{V}}}(t) w_{i_{\mathcal{V}}}(\mathbf{X}).$$

118 The domain at time t is then defined by

$$119 \quad \Omega(t) = \{\mathbf{x} \in \mathbb{R}^d \text{ such that } \exists \mathbf{X} \in \Omega_0 : \mathbf{x} = \Phi(\mathbf{X}, t)\}$$

120 where Φ is given by (2a).

121 The velocity field is approximated by:

$$122 \quad (2b) \quad \mathbf{u}(\mathbf{x}, t) = \sum_{i_{\mathcal{V}} \in \mathcal{D}_{\mathcal{V}}} \mathbf{u}_{i_{\mathcal{V}}}(t) w_{i_{\mathcal{V}}}(\mathbf{X}),$$

123 and the specific internal energy is given by:

$$124 \quad (2c) \quad \varepsilon(\mathbf{x}, t) = \sum_{i_{\mathcal{E}} \in \mathcal{D}_{\mathcal{E}}} \varepsilon_{i_{\mathcal{E}}}(t) \phi_{i_{\mathcal{E}}}(\mathbf{X}).$$

125 Considering the weak formulation of (1), we get:

126 1. For the velocity equation, for any $i_{\mathcal{V}} \in \mathcal{D}_{\mathcal{V}}$,

$$127 \quad (2d) \quad \int_{\Omega_t} \rho \frac{d\mathbf{u}}{dt} w_{i_{\mathcal{V}}} d\mathbf{x} = - \int_{\Omega_t} \boldsymbol{\tau} : \nabla_{\mathbf{x}} w_{i_{\mathcal{V}}} d\mathbf{x} + \int_{\partial\Omega_t} \mathbf{n} \cdot \boldsymbol{\tau} \cdot w_{i_{\mathcal{V}}} d\sigma$$

128 where for now, the stress tensor $\boldsymbol{\tau}$ is defined as $\boldsymbol{\tau} = -p\mathbf{Id}$.²

129 Using (2b), we get³

$$130 \quad \sum_{j_{\mathcal{V}}} \left(\int_{\Omega_t} \rho w_{j_{\mathcal{V}}} w_{i_{\mathcal{V}}} d\mathbf{x} \right) \frac{d\mathbf{u}_{i_{\mathcal{V}}}}{dt} = - \int_{\Omega_t} \boldsymbol{\tau} : \nabla_{\mathbf{x}} w_{i_{\mathcal{V}}} d\mathbf{x} + \int_{\partial\Omega_t} \mathbf{n} \cdot \boldsymbol{\tau} \cdot w_{i_{\mathcal{V}}} d\sigma.$$

131 Introducing the vector $\hat{\mathbf{u}}$ with components $\mathbf{u}_{i_{\mathcal{V}}}$ and \mathbf{F} the force vector given
132 by the right-hand side of the above equation, we get the formulation

$$133 \quad \mathbf{M}_{\mathcal{V}} \frac{d\hat{\mathbf{u}}}{dt} = \mathbf{F}.$$

134 The kinematic mass matrix $\mathbf{M}_{\mathcal{V}} = (M_{i_{\mathcal{V}}j_{\mathcal{V}}}^{\mathcal{V}})$ has components

$$135 \quad M_{i_{\mathcal{V}}j_{\mathcal{V}}}^{\mathcal{V}} = \int_{\Omega_t} \rho w_{j_{\mathcal{V}}} w_{i_{\mathcal{V}}} d\mathbf{x}.$$

136 Thanks to the Reynolds transport theorem (1c) and mass conservation, $\mathbf{M}_{\mathcal{V}}$
137 does not depend on time, see [15] for details.

138 2. For the internal energy, we get a similar form,

$$139 \quad (2e) \quad \int_{\Omega_t} \rho \frac{d\varepsilon}{dt} \phi_{i_{\mathcal{E}}} d\mathbf{x} = \int_{\Omega_t} \phi_{i_{\mathcal{E}}} \boldsymbol{\tau} : \nabla_{\mathbf{x}} \mathbf{u} d\mathbf{x},$$

140 which leads to

$$141 \quad \mathbf{M}_{\mathcal{E}} \frac{d\hat{\boldsymbol{\varepsilon}}}{dt} = \mathbf{W},$$

142 where $\hat{\boldsymbol{\varepsilon}}$ is the vector with components $\varepsilon_{i_{\mathcal{E}}}$, the thermodynamic mass matrix
143 $\mathbf{M}_{\mathcal{E}} = (M_{i_{\mathcal{E}}j_{\mathcal{E}}}^{\mathcal{E}})$ with entries $M_{i_{\mathcal{E}}j_{\mathcal{E}}}^{\mathcal{E}} = \int_{\Omega_t} \phi_{i_{\mathcal{E}}} \phi_{j_{\mathcal{E}}} d\mathbf{x}$ is again independent of
144 time and \mathbf{W} is the right-hand side of (2e).

145 3. The mass satisfies:

$$146 \quad (2f) \quad \det \mathbb{J}(\mathbf{x}, t) \rho(\mathbf{x}, t) = \rho_0(\mathbf{X})$$

147 where $\rho_0 \in \mathcal{E}$. The deformation tensor \mathbb{J} is evaluated according to (2a).

²Here, if \mathbf{X} is a tensor and \mathbf{y} is a vector, $\mathbf{X} \cdot \mathbf{y}$ is the usual matrix-vector multiplication.

³Here, if \mathbf{X} and \mathbf{Y} are tensors, $\mathbf{X} : \mathbf{Y}$ is the contraction $\mathbf{X} : \mathbf{Y} = \text{trace}(\mathbf{X}^T \mathbf{Y})$.

148 4. The positions $\mathbf{x}_{i_{\mathcal{V}}}$ satisfy:

$$149 \quad (2g) \quad \frac{d\mathbf{x}_{i_{\mathcal{V}}}}{dt} = \mathbf{u}_{i_{\mathcal{V}}}(\mathbf{x}_{i_{\mathcal{V}}}, t)$$

150 It remains to define the spaces \mathcal{V} and \mathcal{E} . To do this, we consider a *conformal*
 151 triangulation of the initial computational domain $\Omega_0 \subset \mathbb{R}^d$, $d = 1, 2, 3$, which we shall
 152 denote by \mathcal{T}_h . We denote by K any element of \mathcal{T}_h and assume for simplicity that
 153 $\cup_K K = \Omega_0$. The set of boundary faces is denoted by \mathcal{B} and a generic boundary face is
 154 denoted by f , thus $\cup_{f \in \mathcal{B}} f = \partial\Omega_0$. As usual, denoting by $\mathbb{P}^r(K)$ the set of polynomials
 155 of degree r defined on K , we consider two functional spaces (with integer $r \geq 1$):

$$156 \quad \mathcal{V} = \{\mathbf{v} \in L^2(\Omega_0)^d, \forall K, \mathbf{v}|_K \in \mathbb{P}^r(K)^d\} \cap C^0(\Omega_0)$$

157 and

$$158 \quad \mathcal{E} = \{\theta \in L^2(\Omega_0), \forall K, \theta|_K \in \mathbb{P}^{r-1}(K)\}.$$

159 Clearly, for any t , $x \in \Omega_t$, the Jacobian J is a priori not continuous across the
 160 faces of elements, and hence the relation (2f) is to be understood in the interior of
 161 elements. The matrix $\mathbf{M}_{\mathcal{E}}$ is symmetric positive definite block-diagonal while $\mathbf{M}_{\mathcal{V}}$ is
 162 only a *sparse* symmetric positive definite matrix.

163 The fundamental assumption made here is that the mapping Φ is bijective. In
 164 numerical situations, this can be hard to achieve for long term simulations, and thus
 165 mesh remapping and recomputation of the matrices $\mathbf{M}_{\mathcal{E}}$ and $\mathbf{M}_{\mathcal{V}}$ must be done from
 166 time to time; this issue is however outside of the scope of this paper, see [23] for
 167 detailed discussion.

168 The scheme defined by (2) is only linearly stable. Since we are looking for possibly
 169 discontinuous solutions, in the original scheme of Dobrev et al. a mechanism of arti-
 170 ficial viscosity is added. The idea amounts to modifying the stress tensor $\boldsymbol{\tau} = -p\mathbf{Id}_d$
 171 by $\boldsymbol{\tau} = -p\mathbf{Id}_d + \boldsymbol{\tau}_a(\mathbf{x}, t)$, where the term $\boldsymbol{\tau}_a(\mathbf{x}, t)$ specifies the artificial viscosity. We
 172 refer to [15] for details on the construction of $\boldsymbol{\tau}_a(\mathbf{x}, t)$.

173 It is possible to rewrite the system (1), and in particular the relations (2d) and
 174 (2e) in a slightly different way. Let K be any element of the triangulation \mathcal{T}_h , and for
 175 the kinematic degrees of freedom $i_{\mathcal{V}} \in \mathcal{D}_{\mathcal{V}}$ and the thermodynamic degrees of freedom
 176 $i_{\mathcal{E}} \in \mathcal{D}_{\mathcal{E}}$ consider the quantities

$$177 \quad \Phi_{\mathcal{V}, i_{\mathcal{V}}}^K = \int_K \boldsymbol{\tau} : \nabla_{\mathbf{x}} w_{i_{\mathcal{V}}} d\mathbf{x} - \int_{\partial K} \hat{\boldsymbol{\tau}}_{\mathbf{n}} w_{i_{\mathcal{V}}} d\sigma,$$

$$178 \quad \Phi_{\mathcal{E}, i_{\mathcal{E}}}^K = - \int_K \phi_{i_{\mathcal{E}}}^K \boldsymbol{\tau} : \nabla_{\mathbf{x}} \mathbf{u} d\mathbf{x},$$

$$179$$

180 where $\hat{\boldsymbol{\tau}}_{\mathbf{n}}$ is any numerical flux consistent with $\boldsymbol{\tau} \cdot \mathbf{n}$, see e. g. [24].

181 Using the compactness of the support of the basis functions $w_{i_{\mathcal{V}}}$ and $\phi_{i_{\mathcal{E}}}$, we can
 182 rewrite the relations (2d) and (2e) as follows:

$$183 \quad (3a) \quad \int_{\Omega_t} \rho \frac{d\mathbf{u}}{dt} w_{i_{\mathcal{V}}} d\mathbf{x} + \sum_{K \ni i_{\mathcal{V}}} \Phi_{\mathcal{V}, i_{\mathcal{V}}}^K = 0$$

184 and

$$185 \quad (3b) \quad \int_{\Omega_t} \rho \frac{d\varepsilon}{dt} \phi_{i_{\mathcal{E}}} d\mathbf{x} + \sum_{K \ni i_{\mathcal{E}}} \Phi_{\mathcal{E}, i_{\mathcal{E}}}^K = 0,$$

186 and we notice that on each element K , we have:

187

$$\begin{aligned}
188 \quad (3c) \quad & \sum_{i_\varepsilon \in K} \Phi_{\mathcal{E}, i_\varepsilon}^K + \sum_{i_\nu \in K} \mathbf{u}_{i_\nu} \cdot \Phi_{\mathcal{V}, i_\nu}^K \\
189 \quad & = - \sum_{i_\varepsilon \in K} \int_K \phi_{i_\varepsilon}^K \boldsymbol{\tau} : \nabla_{\mathbf{x}} \mathbf{u} \, d\mathbf{x} + \sum_{i_\nu \in K} \left(\mathbf{u}_{i_\nu} \cdot \int_K \boldsymbol{\tau} : \nabla_{\mathbf{x}} w_{i_\nu} \, d\mathbf{x} - \mathbf{u}_{i_\nu} \cdot \int_{\partial K} \hat{\boldsymbol{\tau}}_{\mathbf{n}} w_{i_\nu} \, d\sigma \right) \\
190 \quad & = - \int_K \boldsymbol{\tau} : \nabla_{\mathbf{x}} \mathbf{u} \, d\mathbf{x} + \int_K \boldsymbol{\tau} : \nabla_{\mathbf{x}} \mathbf{u} \, d\mathbf{x} - \int_{\partial K} \hat{\boldsymbol{\tau}}_{\mathbf{n}} \cdot \mathbf{u} \, d\sigma = - \int_{\partial K} \hat{\boldsymbol{\tau}}_{\mathbf{n}} \cdot \mathbf{u} \, d\sigma. \\
191
\end{aligned}$$

192 There is no ambiguity in the definition of the last integral in (3c) because \mathbf{u} is
193 continuous across ∂K and the numerical flux $\hat{\boldsymbol{\tau}}_{\mathbf{n}}$ is well defined.

194 Since we have the relation (3c) and a similar relation for the total momentum,
195 namely

$$196 \quad (4) \quad \sum_{i_\nu \in K} \Phi_{\mathcal{V}, i_\nu}^K = - \int_{\partial K} \boldsymbol{\tau} \cdot \mathbf{n} \, d\sigma,$$

197 and since the flux $\hat{\boldsymbol{\tau}}_{\mathbf{n}}$ is consistent with $\boldsymbol{\tau} \cdot \mathbf{n}$, one can easily show using the same
198 argument as in [4] that:

- 199 1. if we use a sequence of meshes which typical mesh size tends to 0, while
200 staying shape regular in the sense of classical finite element,
- 201 2. if the numerical solution stay component-wise bounded in L^∞ , converges
202 (component-wise) in L^2 towards some function (\mathbf{u}, e)

203 then this solution is a weak solution of the initial problem.

204 In addition, we have a positive balance of entropy as soon as $\boldsymbol{\tau}_a : \nabla u \geq 0$ in each
205 element since

$$\begin{aligned}
207 \quad \int_K \rho T \frac{ds}{dt} \, d\mathbf{x} & = \int_K \rho \left(\frac{d\varepsilon}{dt} + p \frac{d(1/\rho)}{dt} \right) \, d\mathbf{x} \\
208 \quad & = \int_K \left(\rho \frac{d\varepsilon}{dt} + p \nabla_{\mathbf{x}} \mathbf{u} \right) \, d\mathbf{x} = \int_K (\boldsymbol{\tau}_a : \nabla_{\mathbf{x}} \mathbf{u}) \, d\mathbf{x} \geq 0. \\
209
\end{aligned}$$

210 **4. Residual distribution formulation.** In this section, we briefly recall the
211 concept of residual distribution schemes for the following problem in $\Omega \subset \mathbb{R}^d$:

$$212 \quad \frac{\partial u}{\partial t} + \nabla_{\mathbf{x}} \cdot \mathbf{f}(u) = 0$$

213 with the initial condition $u(\mathbf{x}, 0) = u_0(\mathbf{x})$. For simplicity we assume that u is a real-
214 valued function. Again, we consider a triangulation \mathcal{T}_h of Ω . We want to approximate
215 u in

$$216 \quad V_h = \{u \in L^2(\Omega), \text{ for any } K \in \mathcal{T}_h, u|_K \in \mathbb{P}^r\} \cap C^0(\Omega).$$

217 The set $\{\varphi_i\}$ is a basis of V_h , and u_i are such that $u = \sum_i u_i \varphi_i$. As usual, h represents
218 the maximal diameter of the element of \mathcal{T}_h . We use the same notations as before, and
219 here the index i denotes a generic degree of freedom.

220 We start by the steady version of this problem,

$$221 \quad \nabla_{\mathbf{x}} \cdot \mathbf{f}(u) = 0$$

222 and omit, for the sake of simplicity, the boundary conditions, see [1] for details. We
223 consider schemes of the form:

$$224 \quad (5) \quad \sum_{K \ni i} \Phi_i^K(u) = 0 \quad \forall i,$$

225 with

$$226 \quad \Phi_i^K(u) = \int_K \varphi_i \nabla_{\mathbf{x}} \cdot \mathbf{f}(u) d\mathbf{x}.$$

227 The residuals must satisfy the conservation relation: for any K ,

$$228 \quad (6) \quad \sum_{i \in K} \Phi_i^K(u) = \int_{\partial K} \mathbf{f}^h \cdot \mathbf{n} d\sigma := \Phi^K(u).$$

229 Here, $\mathbf{f}^h \cdot \mathbf{n}$ is an $(r + 1)$ -th order approximation of $\mathbf{f}(u) \cdot \mathbf{n}$. Given a sequence of
 230 meshes that are shape regular with $h \rightarrow 0$, one can construct a sequence of solution.
 231 In [4], it is shown that , if (i) this sequence of solutions stays bounded in L^∞ , (ii)
 232 a subsequence of it converges in $L^2(\Omega)$ towards a limit u and (iii) the residuals are
 233 continuous with respect to u^h , then the conservation condition garanties that u is a
 234 weak solution of the problem.

235 A typical example of such residual is the Rusanov residual,

$$236 \quad \Phi_i^{K,\text{Rus}}(u^h) = - \int_K \nabla_{\mathbf{x}} \varphi_i \cdot \mathbf{f}^h d\mathbf{x} + \int_{\partial K} \mathbf{f}^h \cdot \mathbf{n} \varphi_i d\sigma + \alpha_K(u_i - \bar{u}_K),$$

237 where

$$238 \quad \bar{u}_K = \frac{1}{N_K} \sum_{j \in K} u_j$$

239 with N_K being the number of degrees of freedom inside an element K and

$$240 \quad \alpha_K \geq \max_{\mathbf{x} \in K} \|\mathbf{f}'(u^h)\|.$$

241 This residual can be rewritten as

$$242 \quad \Phi_i^{K,\text{Rus}}(u^h) = \sum_{j \in K} c_{ij}^K(u_i - u_j)$$

243 with $c_{ji}^K \geq 0$. It is easy to see that using the Rusanov residual leads to very dissipative
 244 solutions, but the scheme is easily shown to be monotonicity preserving. There is a
 245 systematic way of improving the accuracy. One can show [4] that if the residuals
 246 satisfy, for any degree of freedom i ,

$$247 \quad \Phi_i^K(u_{ex}^h) = O(h^{k+d}),$$

248 where u_{ex} is the exact solution of the steady problem, u_{ex}^h is an interpolation of order
 249 $k + 1$ and d is the dimension of the problem, then the scheme is formally of order
 250 $k + 1$. It is shown in [4] how to achieve a high order of accuracy while keeping the
 251 monotonicity preserving property. A systematic way of achieving this is to set:

$$252 \quad (7) \quad \Phi_i^K(u) = \beta_i^K(u) \Phi^K(u),$$

253 where

$$254 \quad (8) \quad \beta_i^K(u) = \frac{\max\left(\frac{\Phi_i^{K,\text{Rus}}}{\Phi^K}, 0\right)}{\sum_{j \in K} \max\left(\frac{\Phi_j^{K,\text{Rus}}}{\Phi^K}, 0\right)}$$

255 and Φ^K is defined by (6). Some refinements exist in order to get an entropy inequality,
 256 see [3, 1] for example. Note that $\beta_i^K(u)$ is constant on K .

257 It is easy to see that one can rewrite (7) in a Petrov-Galerkin fashion:

$$258 \quad \Phi_i^K(u) = \int_K \beta_i^K(u) \nabla_{\mathbf{x}} \cdot \mathbf{f}^h \, d\mathbf{x} = \int_K \varphi_i \nabla_{\mathbf{x}} \cdot \mathbf{f}^h \, d\mathbf{x} + \int_K (\beta_i^K(u) - \varphi_i) \nabla_u f \cdot \nabla_{\mathbf{x}} u \, d\mathbf{x}$$

$$259 \quad = - \int_K \nabla_{\mathbf{x}} \varphi_i \cdot \mathbf{f} \, d\mathbf{x} + \int_{\partial K} \varphi_i \mathbf{f} \cdot \mathbf{n} \, d\sigma + \int_K (\beta_i^K(u) - \varphi_i) \nabla_u \mathbf{f} \cdot \nabla_{\mathbf{x}} u \, d\mathbf{x},$$

262 so that from (5) we get

$$263 \quad 0 = - \int_{\Omega} \nabla_{\mathbf{x}} \varphi_i \cdot \mathbf{f} \, d\mathbf{x} + \int_{\partial\Omega} \varphi_i \mathbf{f}(u^h) \cdot \mathbf{n} \, d\sigma + \sum_{K \ni i} \int_K (\beta_i^K(u) - \varphi_i) \nabla_u \mathbf{f} \cdot \nabla_{\mathbf{x}} u \, d\mathbf{x}.$$

264 Inspired by this formulation, we would naturally discretize the unsteady problem
 265 as:

$$266 \quad (9) \quad 0 = \int_{\Omega} \varphi_i \frac{\partial u}{\partial t} \, d\mathbf{x} - \int_{\Omega} \nabla_{\mathbf{x}} \varphi_i \cdot \mathbf{f} \, d\mathbf{x} + \int_{\partial\Omega} \varphi_i \mathbf{f}(u^h) \cdot \mathbf{n} \, d\sigma$$

$$267 \quad + \sum_{i \ni K} \int_K (\beta_i^K(u) - \varphi_i) \left(\frac{\partial u}{\partial t} + \nabla_u \mathbf{f} \cdot \nabla_{\mathbf{x}} u \right) \, d\mathbf{x}.$$

268 The formulation (9) can be as well derived from (5) by introducing the "space-
 271 time" residuals (the value of β_i^K is not relevant at this stage)

$$272 \quad (10) \quad \Phi_i^K(u) = \beta_i^K(u) \int_K \left(\frac{\partial u}{\partial t} + \nabla_{\mathbf{x}} \cdot \mathbf{f}(u^h) \right) \, d\mathbf{x}.$$

273 The semi-discrete scheme (9) requires an appropriate ODE solver for time-stepping.

274 A straightforward discretization of (9) would lead to a mass matrix $\mathbf{M} = (M_{ij})_{i,j}$
 275 with entries

$$276 \quad M_{ij} = \int_{\Omega} \varphi_i \varphi_j \, d\mathbf{x} + \sum_{i \ni K} \int_K (\beta_i^K(u) - \varphi_i) \varphi_j \, d\mathbf{x}.$$

277 Unfortunately, this matrix has no special structure, might not be invertible (so the
 278 problem is not even well posed!), and in any case it is highly non linear since β_i^K
 279 depends on u . A solution to circumvent the problem has been proposed in [21].
 280 The main idea is to keep the spatial structure of the scheme and slightly modify the
 281 temporal one without violating the formal accuracy. A second order version of the
 282 method is designed in [21] and extension to high order is explained in [2]. For the
 283 purposes of this paper and for comparison with [15] we only need the second order
 284 case.

285 Here we describe the idea of the modified time stepping from [21]. We start with
 286 the description of our time-stepping algorithm based on a second order Runge-Kutta
 287 scheme for an ODE of the form

$$288 \quad y' + L(y) = 0.$$

289 Given an approximate solution y_n at time t^n , for the calculation of y_{n+1} we
 290 proceed as follows:

291 1. set $y^{(0)} = y^n$;

292 2. compute $y^{(1)}$ defined by

$$293 \quad \frac{y^{(1)} - y^{(0)}}{\Delta t} + L(y^{(0)}) = 0;$$

294 3. compute $y^{(2)}$ defined by

$$295 \quad \frac{y^{(2)} - y^{(0)}}{\Delta t} + \frac{L(y^{(0)}) + L(y^{(1)})}{2} = 0;$$

296 4. set $y^{n+1} = y^{(2)}$.

297 We see that the generic step in this scheme has the form

$$298 \quad \frac{\delta^k y}{\Delta t} + \mathcal{L}(y^{(0)}, y^{(k)}) = 0$$

299 with

$$300 \quad \mathcal{L}(a, b) = \frac{L(a) + L(b)}{2}$$

301 and

$$302 \quad \delta^k y = y^{(k+1)} - y^{(0)}, \quad k = 0, 1.$$

303 Coming back to the residuals (10), we write for each element K and $k = 0, 1$:

304

$$\begin{aligned} 305 \quad & \beta_i^K(u) \int_K \left(\frac{\delta^k u}{\Delta t} + \mathcal{L}(u^{(0)}, u^{(k)}) \right) d\mathbf{x} \\ 306 \quad & = \int_K \varphi_i \left(\frac{\delta^k u}{\Delta t} + \mathcal{L}(u^{(0)}, u^{(k)}) \right) d\mathbf{x} + \int_K (\beta_i^K(u) - \varphi_i) \left(\frac{\delta^k u}{\Delta t} + \mathcal{L}(u^{(0)}, u^{(k)}) \right) d\mathbf{x} \\ 307 \quad & \approx \int_K \varphi_i \left(\frac{\delta^k u}{\Delta t} + \mathcal{L}(u^{(0)}, u^{(k)}) \right) d\mathbf{x} + \int_K (\beta_i^K(u) - \varphi_i) \left(\frac{\widetilde{\delta^k u}}{\Delta t} + \mathcal{L}(u^{(0)}, u^{(k)}) \right) d\mathbf{x} \\ 308 \end{aligned}$$

309 with

$$310 \quad \widetilde{\delta^k u} = \begin{cases} 0 & \text{if } k = 0, \\ u^{(1)} - u^{(0)} & \text{if } k = 1. \end{cases}$$

311 We see that

312

$$\begin{aligned} 313 \quad & \int_K \varphi_i \left(\frac{\delta^k u}{\Delta t} + \mathcal{L}(u^{(0)}, u^{(k)}) \right) d\mathbf{x} + \int_K (\beta_i^K(u) - \varphi_i) \left(\frac{\widetilde{\delta^k u}}{\Delta t} + \mathcal{L}(u^{(0)}, u^{(k)}) \right) d\mathbf{x} \\ 314 \quad & = \int_K \varphi_i \left(\frac{\delta^k u}{\Delta t} - \frac{\widetilde{\delta^k u}}{\Delta t} \right) d\mathbf{x} + \beta_i^K(u) \int_K \left(\frac{\widetilde{\delta^k u}}{\Delta t} + \mathcal{L}(u^{(0)}, u^{(k)}) \right) d\mathbf{x}. \\ 315 \end{aligned}$$

316 This relation is further simplified if mass lumping can be applied: letting

$$317 \quad (11) \quad C_i^K = \sum_{j \in K} \int_K \varphi_i \varphi_j d\mathbf{x} = \int_K \varphi_i d\mathbf{x}$$

318 and

$$319 \quad (12) \quad C_i = \int_{\Omega} \varphi_i d\mathbf{x} = \sum_{k \ni i} \int_K \varphi_i d\mathbf{x},$$

350 **5. Residual distribution scheme for Lagrangian hydrodynamics.** In this
 351 section, we explain how to adapt the previous framework to the equations of La-
 352 grangian hydrodynamics. We consider the same functional spaces as in section 3,
 353 namely the kinematic space \mathcal{V} and the thermodynamic space \mathcal{E} .

354 In the case of a simplex $K \subset \mathbb{R}^d$, one can consider the barycentric coordinates as-
 355 sociated to the vertices of K and denoted by $\{\Lambda_j\}_{j=1,d+1}$. By definition, the barycen-
 356 tric coordinates are positive on K and we can consider the Bézier polynomials of
 357 degree r : define $r = i_1 + \dots + i_{d+1}$, then

$$358 \quad (16) \quad B_{i_1 \dots i_{d+1}} = \frac{r!}{i_1! \dots i_{d+1}!} \Lambda_1^{i_1} \dots \Lambda_{d+1}^{i_{d+1}}.$$

359 Clearly, $B_{i_1 \dots i_{d+1}} \geq 0$ on K and

$$360 \quad \sum_{i_1, \dots, i_{d+1}, \sum_{j=1}^{d+1} i_j = r} B_{i_1 \dots i_{d+1}} = \left(\sum_{i=1}^{d+1} \Lambda_i \right)^r = 1.$$

361 It is left to define the residuals for the equations of the Lagrangian hydrodynamics.
 362 Since the PDE on the velocity is written in conservation form, this is only a mild
 363 adaptation of the derivations presented in the previous section, at least in the 1D
 364 case when the velocity is a scalar. In the multidimensional case, one can follow [21].
 365 However, we need to introduce some modifications for the thermodynamics. To this
 366 end, we first focus on the spatial term, in the spirit of [21, 3]. We construct a first
 367 order monotone scheme, and using the technique of [3], we design a formally high
 368 order accurate scheme. Therefore, we introduce the total residuals

$$369 \quad (17) \quad \Phi^K = \int_{\partial K} \hat{p}_n d\sigma \quad \text{and} \quad \Psi^K = \int_K p \nabla_{\mathbf{x}} \cdot \mathbf{u} d\mathbf{x},$$

370 where $p \in \mathcal{E}$, $\mathbf{u} \in \mathcal{V}$ and \hat{p}_n is a consistent numerical flux which depends on the left
 371 and right state at ∂K . Next, the Galerkin residuals are given by

$$372 \quad (18) \quad \begin{aligned} \Phi_{i_{\mathcal{V}}}^K &= - \int_K p \nabla_{\mathbf{x}} \phi_{i_{\mathcal{V}}} d\mathbf{x} + \int_{\partial K} \phi_{i_{\mathcal{V}}} \hat{p}_n d\sigma, \\ \Psi_{i_{\mathcal{E}}}^K &= \int_K \psi_{i_{\mathcal{E}}} p \nabla_{\mathbf{x}} \cdot \mathbf{u} d\mathbf{x}. \end{aligned}$$

373 From (18), we define the Rusanov residuals

$$374 \quad (19) \quad \Phi_{i_{\mathcal{V}}}^{K, \text{Rus}}(\mathbf{u}, \varepsilon) = \Phi_{i_{\mathcal{V}}}^K(\mathbf{u}, \varepsilon) + \alpha_K(\mathbf{u}_{i_{\mathcal{V}}} - \bar{\mathbf{u}}), \quad \bar{\mathbf{u}} = \frac{1}{N_{\mathcal{V}}^K} \sum_{i_{\mathcal{V}} \in K} \mathbf{u}_{i_{\mathcal{V}}}$$

375 and

$$376 \quad (20) \quad \Psi_{i_{\mathcal{E}}}^{K, \text{Rus}}(\mathbf{u}, \varepsilon) = \Psi_{i_{\mathcal{E}}}^K(\mathbf{u}, \varepsilon) + \alpha_K(\varepsilon_{i_{\mathcal{E}}} - \bar{\varepsilon}), \quad \bar{\varepsilon} = \frac{1}{N_{\mathcal{E}}^K} \sum_{i_{\mathcal{E}} \in K} \varepsilon_{i_{\mathcal{E}}}$$

377 where α_K is an upper bound of the Lagrangian speed of sound ρc on K and $N_{\mathcal{V}}^K$
 378 (resp. $N_{\mathcal{E}}^K$) is the number of degrees of freedom for the velocity (resp. energy) on K .

379 The temporal discretization is done using the technique developed in the previous
 380 section. We introduce the modified space-time Rusanov residuals, for $k = 0, 1$:

$$381 \quad (21) \quad \Phi_{i_{\mathcal{V}}, ts}^{K, \text{Rus}} = \int_K \varphi_{i_{\mathcal{V}}} \rho \frac{\delta^k \mathbf{u}}{\Delta t} d\mathbf{x} + \frac{1}{2} \left(\Phi_{i_{\mathcal{V}}}^{K, \text{Rus}}(\mathbf{u}^{(0)}, \varepsilon^{(0)}) + \Phi_{i_{\mathcal{V}}}^{K, \text{Rus}}(\mathbf{u}^{(k)}, \varepsilon^{(k)}) \right)$$

382 and

$$383 \quad (22) \quad \Psi_{i_\varepsilon, ts}^{K, \text{Rus}} = \int_K \psi_{i_\varepsilon} \rho \frac{\widetilde{\delta^k \varepsilon}}{\Delta t} d\mathbf{x} + \frac{1}{2} \left(\Psi_{i_\varepsilon}^{K, \text{Rus}}(\mathbf{u}^{(0)}, \varepsilon^{(0)}) + \Psi_{i_\varepsilon}^{K, \text{Rus}}(\mathbf{u}^{(k)}, \varepsilon^{(k)}) \right).$$

384 Finally, the high-order limited residuals are computed similarly to (7) as

$$385 \quad (23) \quad \Phi_{i_\nu, ts}^{K, L} = \beta_{i_\nu}^K \Phi_{ts}^K, \quad \Psi_{i_\varepsilon, ts}^{K, L} = \beta_{i_\varepsilon}^K \Psi_{ts}^K,$$

386 where the space-time Rusanov residuals (21) and (22) are used in expressions analo-
387 gous to (8) to calculate $\beta_{i_\nu}^K$ and $\beta_{i_\varepsilon}^K$, respectively:

$$388 \quad (24) \quad \beta_{i_\nu}^K = \frac{\max\left(\frac{\Phi_{i_\nu, ts}^{K, \text{Rus}}}{\Phi_{ts}^K}, 0\right)}{\sum_{j_\nu \in K} \max\left(\frac{\Phi_{j_\nu, ts}^{K, \text{Rus}}}{\Phi_{ts}^K}, 0\right)},$$

389

$$390 \quad (25) \quad \beta_{i_\varepsilon}^K = \frac{\max\left(\frac{\Psi_{i_\varepsilon, ts}^{K, \text{Rus}}}{\Psi_{ts}^K}, 0\right)}{\sum_{j_\varepsilon \in K} \max\left(\frac{\Psi_{j_\varepsilon, ts}^{K, \text{Rus}}}{\Psi_{ts}^K}, 0\right)},$$

391 and

$$392 \quad \Phi_{ts}^K = \sum_{i_\nu \in K} \Phi_{i_\nu, ts}^{K, \text{Rus}} = \int_K \left(\rho \frac{\widetilde{\delta^k \mathbf{u}}}{\Delta t} + \frac{1}{2} (\nabla_{\mathbf{x}} p^{(0)} + \nabla_{\mathbf{x}} p^{(k)}) \right) d\mathbf{x},$$

$$393 \quad \Psi_{ts}^K = \sum_{i_\varepsilon \in K} \Psi_{i_\varepsilon, ts}^{K, \text{Rus}} = \int_K \left(\rho \frac{\widetilde{\delta^k \varepsilon}}{\Delta t} + \frac{1}{2} (p^{(0)} \nabla_{\mathbf{x}} \cdot \mathbf{u}^{(0)} + p^{(k)} \nabla_{\mathbf{x}} \cdot \mathbf{u}^{(k)}) \right) d\mathbf{x}.$$

394

395 Next, we introduce

$$396 \quad C_{i_\nu}^{\mathcal{V}, K} = \int_K \rho \varphi_{i_\nu} d\mathbf{x}, \quad C_{i_\varepsilon}^{\mathcal{E}, K} = \int_K \rho \psi_{i_\varepsilon} d\mathbf{x}.$$

397 After applying the mass lumping as in (11), (12), the mass matrices \mathbf{M}_ν for the ve-
398 locity and \mathbf{M}_ε for the thermodynamics become diagonal with entries at the diagonals
399 given by

$$400 \quad C_{i_\nu}^{\mathcal{V}} = \int_\Omega \rho \varphi_{i_\nu} d\mathbf{x} = \sum_{K \ni i_\nu} \int_K \rho \varphi_{i_\nu} d\mathbf{x},$$

$$401 \quad C_{i_\varepsilon}^{\mathcal{E}} = \int_\Omega \rho \psi_{i_\varepsilon} d\mathbf{x} = \sum_{K \ni i_\varepsilon} \int_K \rho \psi_{i_\varepsilon} d\mathbf{x}.$$

402

403 Both matrices are invertible because $\varphi_{i_\nu} > 0$ and $\psi_{i_\varepsilon} > 0$ in the element since
404 we are using Bézier basis. Note that we could have omitted the mass lumping for the
405 thermodynamic relation because the mass matrix is block diagonal.

406 By construction, the scheme is conservative for the velocity, however, nothing
407 is guaranteed for the specific energy. In order to solve this issue, inspired by the

408 calculations of section 3, and given a set of velocity residuals $\{\Phi_{i_\nu}^K\}$ and internal
 409 energy residuals $\{\Psi_{i_\varepsilon}^K\}$, we slightly modify the internal energy evaluation by defining

$$410 \quad (26) \quad \Psi_{i_\varepsilon,ts}^{K,c} = \Psi_{i_\varepsilon,ts}^{K,L} + r_{i_\varepsilon},$$

411 where the correction term r_{i_ε} is chosen to ensure the discrete conservation properties
 412 and will be specified in the following section.

413 With all the above definitions, the resulting residual distribution scheme is written
 414 as follows: for $k = 0, 1$

$$415 \quad (27a) \quad C_{i_\nu}^{\mathcal{V}} \frac{\mathbf{u}_{i_\nu}^{(k+1)} - \mathbf{u}_{i_\nu}^{(k)}}{\Delta t} + \sum_{K \ni i_\nu} \Phi_{i_\nu,ts}^{K,L} = 0,$$

416

$$417 \quad (27b) \quad C_{i_\varepsilon}^{\mathcal{E}} \frac{\varepsilon_{i_\varepsilon}^{(k+1)} - \varepsilon_{i_\varepsilon}^{(k)}}{\Delta t} + \sum_{K \ni i_\varepsilon} \Psi_{i_\varepsilon,ts}^{K,c} = 0,$$

418

$$419 \quad (27c) \quad \frac{\mathbf{x}_{i_\nu}^{(k+1)} - \mathbf{x}_{i_\nu}^n}{\Delta t} = \frac{1}{2} (\mathbf{u}_{i_\nu}^n + \mathbf{u}_{i_\nu}^{(k)}).$$

420 Note that the discretization (27c) is nothing but a second-order SSP RK scheme.

421 **6. Conservation and entropy production.** Here we first derive the expres-
 422 sion for the term r_{i_ε} to ensure the local conservation property of the residual distri-
 423 bution scheme (27) and then give some conditions on the discrete entropy production.

424 **6.1. Discrete conservation.** The continuous problem satisfies the following
 425 conservation property for the specific total energy $e = \frac{1}{2} \mathbf{u}^2 + \varepsilon$:

$$426 \quad (28) \quad \int_K \rho \frac{de}{dt} dx + \int_{\partial K} p \mathbf{u} \cdot \mathbf{n} d\sigma = 0.$$

427 The numerical scheme has to satisfy a conservation property analogous to (28) at
 428 the discrete level. To achieve this, the thermodynamic residual has been modified
 429 according to (26).

430 The term r_{i_ε} is chosen such that:

431

$$432 \quad (29) \quad \sum_{i_\nu \in K} \mathbf{u}_{i_\nu} \left(C_{i_\nu}^{\mathcal{V},K} \left(\frac{\delta^k \mathbf{u}_{i_\nu}}{\Delta t} - \widetilde{\frac{\delta^k \mathbf{u}_{i_\nu}}{\Delta t}} \right) + \Phi_{i_\nu}^{K,L} \right)$$

$$433 \quad + \sum_{i_\varepsilon \in K} \left(C_{i_\varepsilon}^{\mathcal{E},K} \left(\frac{\delta^k \varepsilon_{i_\varepsilon}}{\Delta t} - \widetilde{\frac{\delta^k \varepsilon_{i_\varepsilon}}{\Delta t}} \right) + \Psi_{i_\varepsilon,ts}^{K,L} + r_{i_\varepsilon} \right) = 0.$$

434

435 Since we have only one constraint, we impose in addition that $r_{i_\varepsilon} = r$ for any i_ε ,
 436 so that from (29) we can derive

437

$$438 \quad (30) \quad r_{i_\varepsilon} = \frac{1}{N_\varepsilon^K} \left(\int_{\partial K} \hat{p}_n \mathbf{u} d\sigma - \sum_{i_\nu \in K} \mathbf{u}_{i_\nu} \Phi_{i_\nu}^{K,L} + \sum_{i_\nu \in K} C_{i_\nu}^{\mathcal{V},K} \frac{\widetilde{\delta^k \mathbf{u}_{i_\nu}}}{\Delta t} \right.$$

$$439 \quad \left. - \sum_{i_\varepsilon \in K} \Psi_{i_\varepsilon}^{K,L} + \sum_{i_\varepsilon \in K} C_{i_\varepsilon}^{\mathcal{E},K} \frac{\widetilde{\delta^k \varepsilon_{i_\varepsilon}}}{\Delta t} \right),$$

440

441 where \hat{p}_n is the approximation of the pressure flux $p\mathbf{n}$ at the boundary of the element
442 K .

443 So far, we have indicated a way to recover local conservation by adding a term to
444 the internal energy equation. This term depends on the residuals that are themselves
445 constructed from first order residuals and in turn depend on the pressure flux, so
446 that the conservation property is valid for any pressure flux. It is possible to add
447 further constraints for better conservation properties and in this section we show how
448 to impose a local (semi-discrete) entropy inequality. We also state two results that
449 are behind the construction.

450 **6.2. Entropy balance.** Since at the continuous level

$$451 \quad T \frac{ds}{dt} = \frac{d\varepsilon}{dt} + p \frac{dv}{dt},$$

452 where $v = 1/\rho$ is the specific volume, and knowing that

$$453 \quad \rho \frac{dv}{dt} = \nabla_{\mathbf{x}} \cdot \mathbf{u},$$

454 we look at the entropy inequality

$$455 \quad (31) \quad \int_K \rho T \frac{ds}{dt} = \int_K \rho \left(\frac{d\varepsilon}{dt} + p \frac{dv}{dt} \right) d\mathbf{x} = \int_K \left(\rho \frac{d\varepsilon}{dt} + p \nabla_{\mathbf{x}} \cdot \mathbf{u} \right) d\mathbf{x} \geq 0$$

456 and try to derive its discrete counterpart.

457 For the sake of simplicity we demonstrate the discrete entropy balance conditions
458 on the first-order version of the scheme (27). Taking the sum over the degrees of
459 freedom of an element K in equation (27b) and noting that in the first-order scheme
460 $\widetilde{\delta^k \varepsilon} / \Delta t = 0$ and $\Psi_{i_\varepsilon}^{K,L} = \Psi_{i_\varepsilon}^{K,\text{Rus}}$, we get

$$461 \quad (32) \quad \sum_{i_\varepsilon \in K} C_{i_\varepsilon}^{\varepsilon,K} \frac{\delta^k \varepsilon_{i_\varepsilon}}{\Delta t} + \sum_{i_\varepsilon \in K} \Psi_{i_\varepsilon}^{K,c}$$

$$463 \quad = \sum_{i_\varepsilon \in K} \left(\int_K \rho \psi_{i_\varepsilon} d\mathbf{x} \right) \frac{\delta^k \varepsilon_{i_\varepsilon}}{\Delta t} + \sum_{i_\varepsilon \in K} (\Psi_{i_\varepsilon}^{K,\text{Rus}} + r_{i_\varepsilon}) = \int_K \rho \frac{\delta^k \varepsilon}{\Delta t} d\mathbf{x} + \Psi^K + \sum_{i_\varepsilon \in K} r_{i_\varepsilon}$$

$$464 \quad = \int_K \left(\rho \frac{\delta^k \varepsilon}{\Delta t} + p \nabla_{\mathbf{x}} \cdot \mathbf{u} \right) d\mathbf{x} + \sum_{i_\varepsilon \in K} r_{i_\varepsilon} = 0.$$

465
466 The first term in (32) is a discrete analogue of (31), therefore we can require

$$467 \quad \int_K \left(\rho \frac{\delta^k \varepsilon}{\Delta t} + p \nabla_{\mathbf{x}} \cdot \mathbf{u} \right) d\mathbf{x} \geq 0,$$

468 which yields another constraint on r_{i_ε} :

$$469 \quad (33) \quad \sum_{i_\varepsilon \in K} r_{i_\varepsilon} \leq 0.$$

470 We note that the derivation of the entropy condition for a general high-order scheme
471 is slightly more tedious, however, it leads to exactly the same condition (33) and is
472 therefore not presented here.

473 Let us show that the entropy condition (33) holds for the first order residual
 474 distribution scheme. From the conservation condition (30) we have

$$475 \quad r_{i_\varepsilon} = \frac{1}{N_\varepsilon^K} \left(\int_{\partial K} \hat{p}_n \mathbf{u} d\sigma - \sum_{i_\nu \in K} \mathbf{u}_{i_\nu} \Phi_{i_\nu}^{K, \text{Rus}} - \sum_{i_\varepsilon \in K} \Psi_{i_\varepsilon}^{K, \text{Rus}} \right),$$

476 and therefore

$$477 \quad (34) \quad \sum_{i_\varepsilon \in K} r_{i_\varepsilon} = \int_{\partial K} \hat{p}_n \mathbf{u} d\sigma - \sum_{i_\nu \in K} \mathbf{u}_{i_\nu} \Phi_{i_\nu}^{K, \text{Rus}} - \sum_{i_\varepsilon \in K} \Psi_{i_\varepsilon}^{K, \text{Rus}}$$

$$479 \quad = \int_{\partial K} \hat{p}_n \mathbf{u} d\sigma - \sum_{i_\nu \in K} \mathbf{u}_{i_\nu} \Phi_{i_\nu}^K - \alpha_K \sum_{i_\nu \in K} \mathbf{u}_{i_\nu} (\mathbf{u}_{i_\nu} - \bar{\mathbf{u}}) - \sum_{i_\varepsilon \in K} \Psi_{i_\varepsilon}^K - \alpha_K \sum_{i_\varepsilon \in K} (\varepsilon_{i_\varepsilon} - \bar{\varepsilon})$$

$$480 \quad = \int_{\partial K} \hat{p}_n \mathbf{u} d\sigma - \int_K \mathbf{u} \cdot \nabla_{\mathbf{x}} p d\mathbf{x} - \alpha_K \sum_{i_\nu \in K} (\mathbf{u}_{i_\nu} - \bar{\mathbf{u}})^2 - \int_K p \nabla_{\mathbf{x}} \cdot \mathbf{u} d\mathbf{x}$$

$$481 \quad = -\alpha_K \sum_{i_\nu \in K} (\mathbf{u}_{i_\nu} - \bar{\mathbf{u}})^2 \leq 0,$$

482 where we have taken into account that

$$484 \quad \sum_{i_\nu \in K} \mathbf{u}_{i_\nu} (\mathbf{u}_{i_\nu} - \bar{\mathbf{u}}) = \sum_{i_\nu \in K} (\mathbf{u}_{i_\nu} - \bar{\mathbf{u}})^2, \quad \text{and} \quad \sum_{i_\varepsilon \in K} (\varepsilon_{i_\varepsilon} - \bar{\varepsilon}) = 0.$$

485 Therefore, the entropy condition (33) is satisfied with any $\alpha_K \geq 0$.

486 For high order schemes it doesn't seem to be possible to recast the entropy con-
 487 dition (33) explicitly in terms of α_K as it is done in (34) for the first order scheme
 488 since α_K is only implicitly used to calculate the limiting coefficients $\beta_{i_\nu}^K$ and $\beta_{i_\varepsilon}^K$, by
 489 (24), (25). Therefore, in practice, in order to ensure the entropy inequality in the
 490 high order scheme we add an edge stabilization term to the velocity residual:

$$491 \quad (35) \quad \Phi_{i_\nu}^{K, \text{stab}} = \sum_{e \in \partial K} h^2 \theta \int_e [\nabla_{\mathbf{x}} \cdot \mathbf{u}] [\nabla_{\mathbf{x}} \varphi_{i_\nu}] \cdot \mathbf{n} d\sigma,$$

492 where $\theta > 0$ is a coefficient that can be estimated and $[f] = f^+ - f^-$ is the jump of
 493 f at the interface, see [11] for more details.

494 **6.3. Results on conservation and entropy inequality.** Using the same tech-
 495 nique as in [4], we can easily state the following two results:

496 **PROPOSITION 6.1 (Conservation).** *Assume that we are given a set of regular*
 497 *meshes which characteristic size h tends to zero. Consider the time $t > 0$ so that*
 498 *the meshes mapped by the transformation (1a) stay regular. Assume that the scheme*
 499 *(27), with the residuals defined as in section 5 generate solutions that are bounded in*
 500 *L^∞ by a constant that only depends on the family of meshes and the initial conditions.*
 501 *If a subsequence of these solutions converges towards \mathbf{u} , ε , then this is a weak solution*
 502 *of the Euler equations.*

503 A weak solution satisfies an entropy inequality under certain conditions which are
 504 specified by the following result.

505 **PROPOSITION 6.2 (Entropy).** *If in addition to the assumptions of Proposition 6.1*
 506 *the energy correction satisfies (33), then the limit solution satisfies*

$$507 \quad \rho T \frac{ds}{dt} \geq 0$$

508 *in the sense of distributions.*

509 **7. Second order scheme in one-dimensional case.** In this section, we specify
510 in detail the algorithm of the second order residual distribution scheme in the
511 one-dimensional case. Hereafter, X and x denote the Lagrangian and Eulerian coordinates,
512 respectively, and the scalar velocity is denoted by u .

513 We assume that $X \in [a, b] = \Omega_0$ and introduce a moving grid with nodes x_i ,
514 $i = 0, \dots, N$ and set $K := [x_j, x_{j+1}]$. The kinematic space \mathcal{V} is formed by the
515 continuous quadratic Bézier elements in Ω_0 while the thermodynamic space \mathcal{E} has a
516 piecewise-linear basis. As before, we denote by $\mathcal{D}_{\mathcal{V}}$ (resp. $\mathcal{D}_{\mathcal{E}}$) the set of degrees of
517 freedom in \mathcal{V} (resp. \mathcal{E}).

518 The algorithm of the one-dimensional second order scheme consists of two steps.

519 **Step 1:** calculate $u_h^{(1)}, \varepsilon_h^{(1)}, x_h^{(1)}$. For any $i_{\mathcal{V}} \in \mathcal{D}_{\mathcal{V}}$ and $i_{\mathcal{E}} \in \mathcal{D}_{\mathcal{E}}$

$$\begin{aligned} C_{i_{\mathcal{V}}}^{\mathcal{V}} \frac{u_{i_{\mathcal{V}}}^{(1)} - u_{i_{\mathcal{V}}}^n}{\Delta t} + \sum_{K \ni i_{\mathcal{V}}} \beta_{i_{\mathcal{V}}}^K \int_K \frac{\partial p_h^n}{\partial x} dx &= 0, \\ C_{i_{\mathcal{E}}}^{\mathcal{E}} \frac{\varepsilon_{i_{\mathcal{E}}}^{(1)} - \varepsilon_{i_{\mathcal{E}}}^n}{\Delta t} + \sum_{K \ni i_{\mathcal{E}}} \left[\beta_{i_{\mathcal{E}}}^K \int_K p_h^n \frac{\partial u_h^n}{\partial x} dx + r_{i_{\mathcal{E}}}^{(0)} \right] &= 0, \\ \frac{x_{i_{\mathcal{V}}}^{(1)} - x_{i_{\mathcal{V}}}^n}{\Delta t} &= u_{i_{\mathcal{V}}}^n, \end{aligned}$$

521 where $\beta_{i_{\mathcal{V}}}^K$ (resp. $\beta_{i_{\mathcal{E}}}^K$) is evaluated using (24) (resp. (25)) with $k = 0$, and the
522 correction term $r_{i_{\mathcal{E}}}^{(0)}$ is defined via (30).

523 **Step 2:** calculate $u_h^{n+1}, \varepsilon_h^{n+1}, x_h^{n+1}$. For any $i_{\mathcal{V}} \in \mathcal{D}_{\mathcal{V}}$ and $i_{\mathcal{E}} \in \mathcal{D}_{\mathcal{E}}$,

$$\begin{aligned} C_{i_{\mathcal{V}}}^{\mathcal{V}} \frac{u_{i_{\mathcal{V}}}^{n+1} - u_{i_{\mathcal{V}}}^{(1)}}{\Delta t} + \sum_{K \ni i_{\mathcal{V}}} \beta_{i_{\mathcal{V}}}^K \int_K \left(\rho_h^n \frac{u_h^{(1)} - u_h^n}{\Delta t} + \frac{1}{2} \left(\frac{\partial p_h^n}{\partial x} + \frac{\partial p_h^{(1)}}{\partial x} \right) \right) dx &= 0, \\ C_{i_{\mathcal{E}}}^{\mathcal{E}} \frac{\varepsilon_{i_{\mathcal{E}}}^{n+1} - \varepsilon_{i_{\mathcal{E}}}^{(1)}}{\Delta t} + \sum_{K \ni i_{\mathcal{E}}} \left[\beta_{i_{\mathcal{E}}}^K \int_K \left(\rho_h^n \frac{\varepsilon_h^{(1)} - \varepsilon_h^n}{\Delta t} + \frac{1}{2} \left(p_h^n \frac{\partial u_h^n}{\partial x} + p_h^{(1)} \frac{\partial u_h^{(1)}}{\partial x} \right) \right) dx + r_{i_{\mathcal{E}}}^{(1)} \right] &= 0, \\ \frac{x_{i_{\mathcal{V}}}^{n+1} - x_{i_{\mathcal{V}}}^{(1)}}{\Delta t} &= \frac{1}{2} (u_{i_{\mathcal{V}}}^n + u_{i_{\mathcal{V}}}^{(1)}), \end{aligned}$$

525 where again $\beta_{i_{\mathcal{V}}}^K$ (resp. $\beta_{i_{\mathcal{E}}}^K$) is defined using (24), (resp. (25)) for $k = 1$, and the
526 correction term $r_{i_{\mathcal{E}}}^{(1)}$ is calculated via (30).

527 The density $\rho(x, t)$, when needed, is evaluated via the local relation $\rho(x, t) =$
528 $J(x, t)\rho_0(X)$, where J is the Jacobian of the coordinate transformation, i.e. determinant
529 of the matrix defined by (1b) and ρ_0 is the density in the initial configuration.
530 Note that the mesh is legal as long as J stays strictly positive.

531 **8. Numerical results.** To assess the accuracy and robustness of the proposed
532 residual distribution scheme we solve a series of shock tube problems. For numerical
533 experiments of this section we shall use the following EOS:

- 534 • ideal EOS: $p = (\gamma - 1)\rho\varepsilon$, where $\gamma > 1$,
- 535 • stiffened EOS: $p = (\gamma - 1)\rho\varepsilon - \gamma p_s$,
- 536 • Jones-Wilkins-Lee (JWL) EOS: $p = (\gamma - 1)\rho\varepsilon + f_j(\rho)$, where

$$537 \quad f_j(\rho) = A_1 \left(1 - \frac{(\gamma - 1)\rho}{R_1 \bar{\rho}} \right) \exp \left(- \frac{R_1 \bar{\rho}}{\rho} \right) + A_2 \left(1 - \frac{(\gamma - 1)\rho}{R_1 \bar{\rho}} \right) \exp \left(- \frac{R_1 \bar{\rho}}{\rho} \right).$$

538 If not explicitly specified, the gas is supposed to be modeled by the ideal EOS with
 539 $\gamma = 1.4$.

540 We use the technique proposed in [19] to control the time step and in all numerical
 541 tests the CFL number is set to 0.5.

542 **8.1. Numerical convergence study.** We test the accuracy of our scheme on a
 543 smooth isentropic flow problem similar to the test case introduced in [14]. The initial
 544 data for our test problem is the following:

545
$$\rho_0(x) = 1 + 0.9999995 \sin(2\pi x), \quad u_0(x) = 0, \quad p_0(x) = \rho^\gamma(x, 0), \quad x \in [-1, 1].$$

546 with polytropic index $\gamma = 3$ and periodic boundary conditions.

547 The exact density and velocity in this case can be obtained by the method of
 548 characteristics and is explicitly given by

549
$$\rho(x, t) = \frac{1}{2}(\rho_0(x_1) + \rho_0(x_2)), \quad u(x, t) = \sqrt{3}(\rho(x, t) - \rho_0(x_1)),$$

550 where for each coordinate x and time t the values x_1 and x_2 are solutions of the
 551 nonlinear equations

552
$$x + \sqrt{3}\rho_0(x_1)t - x_1 = 0,$$

 553
$$x - \sqrt{3}\rho_0(x_2)t - x_2 = 0.$$

555 Fig. 1 shows the errors of the flow parameters in the L_1 -norm with respect to the
 556 number of DOFs at time $T = 0.08$ for three different residual distribution schemes
 557 using Bezier basis: first-order RD scheme with modified timestepping and mass lumping
 558 (denoted by "B1/B0"), second-order RD scheme with modified timestepping and
 559 mass lumping ("B2/B1") and the second-order RD scheme with classical second-order
 560 Runge-Kutta timestepping ("B2/B1 RK2"). It can be clearly seen that the first-order
 561 "B1/B0" and second-order "B2/B1" schemes reach the expected convergence rates
 562 while the order of the formally second-order "B2/B1 RK2" scheme drops to first,
 563 which is the result of the loss of accuracy due to mass lumping applied in a standard
 564 timestepping algorithm.

565 **8.2. The Sod shock tube.** The Sod's shock tube is a classical test problem for
 566 the assessment of the numerical methods for solving the Euler equations. Its solution
 567 consists of a left rarefaction, a contact and a right shock wave. The initial data for
 568 this problem is given as follows:

569
$$(\rho_0, u_0, p_0) = \begin{cases} (1.0, 0.0, 1.0), & x < 0, \\ (0.125, 0.0, 0.1), & x > 0. \end{cases}$$

570 The results for first-order ("B1/B0") and second-order ("B2/B1") schemes are
 571 shown in Fig. 2. Obviously, the second-order scheme provides better resolution of
 572 the smooth flow regions such as the left rarefaction wave, while both schemes give an
 573 accurate approximation of the contact discontinuity and the right shock wave.

574 **8.3. 123-problem.** The 123-problem [24] is a classical benchmark case to test
 575 the behaviour of the numerical method for low-density and low-pressure flows. The
 576 initial data is the following:

577
$$(\rho_0, u_0, p_0) = \begin{cases} (1.0, -2.0, 0.4), & -4 \leq x < 0, \\ (1.0, 2.0, 0.4), & 0 < x \leq 4. \end{cases}$$

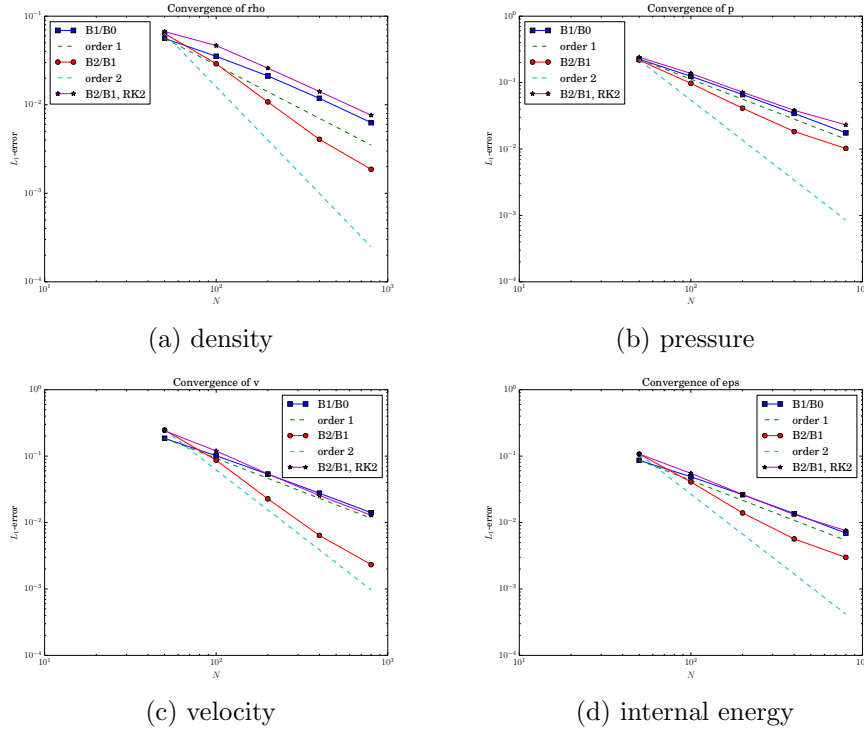


FIG. 1. *Convergence history for the smooth isentropic test problem*

578 The solution of this problem consists of two rarefaction waves traveling in opposite
 579 directions, so that a low-density and low-pressure region is generated in between.

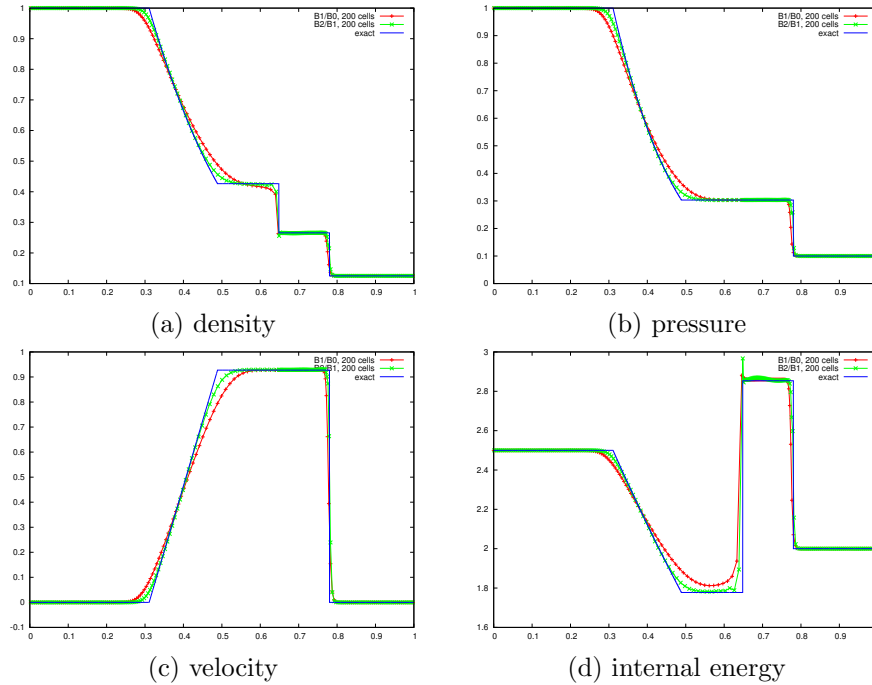
580 The numerical solution illustrated in Fig. 3 shows that the low intermediate density
 581 and pressure are captured correctly by both first-order and second-order RD
 582 scheme, the latter being more accurate for the internal energy. The insufficient resolu-
 583 tion of the flow near the vacuum is a well-known phenomenon for Lagrangian
 584 schemes, and is related to the strong heating phenomenon, see e.g. [14, 26, 27].

585 **8.4. Strong shock.** This test case is actually the left half of the blast wave
 586 problem of Woodward and Colella [30]. It's a severe test problem containing a left
 587 rarefaction wave, a contact discontinuity and a strong right shock wave and it is often
 588 used to assess the robustness of the numerical methods for fluid dynamics [24]. The
 589 initial data for this test problem is

$$590 \quad (\rho_0, u_0, p_0) = \begin{cases} (1.0, 0.0, 1000.0), & x < 0, \\ (1.0, 0.0, 0.01), & x > 0. \end{cases}$$

591 The simulation results shown in Fig. 4 indicate that both first and second-order
 592 schemes are robust and can accurately resolve strong shocks.

593 **8.5. Interaction of blast waves.** The interaction of blast waves is a standard
 594 low energy benchmark problem involving strong shocks reflecting from the walls of


 FIG. 2. Solution of the Sod shock tube problem at $T = 0.16$

595 the tube with further mutual interaction. The initial data is the following:

596
$$\rho_0 = 1, \quad u_0 = 1, \quad p_0 = \begin{cases} 10^3, & 0 \leq x < 0.1, \\ 10^{-2}, & 0.1 < x < 0.9, \\ 10^2, & 0.9 < x \leq 1. \end{cases}$$

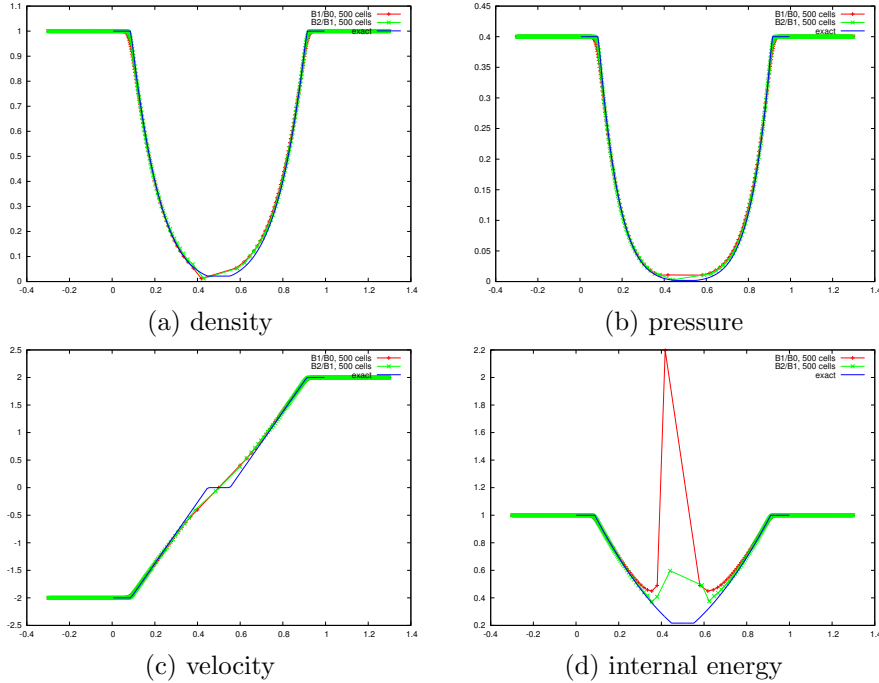
597 Reflective boundary conditions are applied at $x = 0$ and $x = 1$.

598 **8.6. Gas-liquid shock tube.** This severe water-air shock tube problem is used
 599 to assess the performance of the numerical schemes for multi-material flows with a
 600 strong interfacial contact discontinuity. In this problem, the fluid to the left-hand side
 601 of the membrane initially located at $x = 0.3$ is a perfect gas with $\gamma = 1.4$ in the ideal
 602 EOS, while the fluid to the right of the membrane is water modeled by the stiffened
 603 EOS with $\gamma = 4.4$ and $p_s = 6 \cdot 10^8$. The initial parameters of the two fluids are the
 604 following:

605
$$(\rho_0, u_0, p_0) = \begin{cases} (5.0, 0.0, 10^5), & 0 \leq x < 0.3, \\ (10^3, 0.0, 10^9), & 0.3 < x \leq 1. \end{cases}$$

606 The computational results for the first and second-order RD schemes shown in
 607 Fig. 6 demonstrate a very good agreement with the exact solution and, what is im-
 608 portant, a very accurate resolution of the interfacial contact discontinuity by both
 609 schemes.

610 **8.7. Underwater TNT explosion.** This 1D spherically symmetric underwater
 611 detonation problem [18] is often used as a benchmark to test the robustness of the

FIG. 3. Solution of the 123-problem at $T = 0.15$

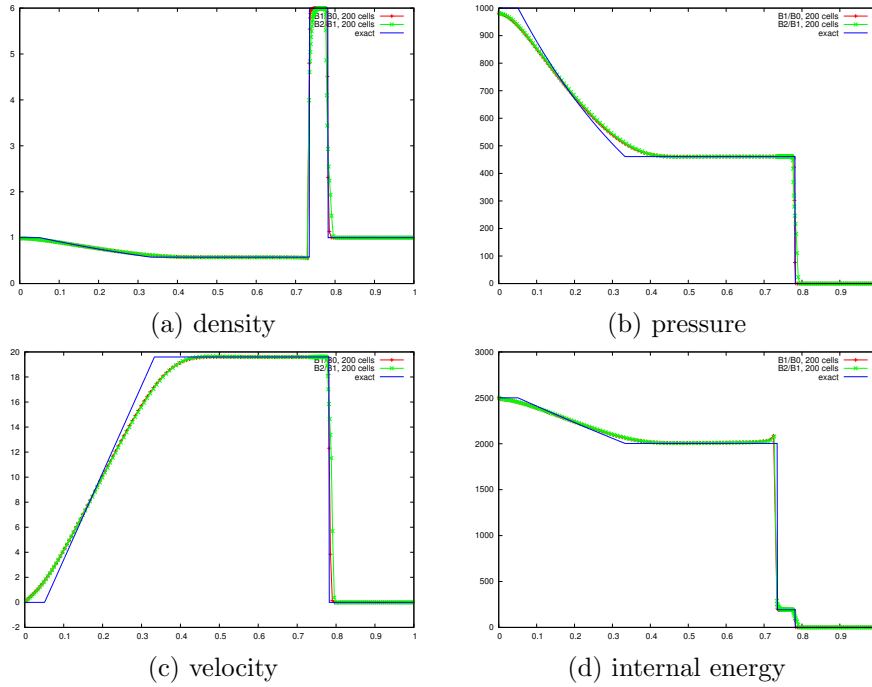
612 methods for multi-phase problems with general equation of state. The initial condition
 613 consists of the detonation products phase on the left of the initial discontinuity and
 614 the water phase to the right. We consider the stiffened version of the classical TNT
 615 explosion problem proposed in [14], which is more likely to produce negative density
 616 and/or internal energy.

617 To the left of the interface initially located at $x = 0.16$, the gaseous product of the
 618 detonated explosive is modeled by the JWLEOS with $A_1 = 3.712 \cdot 10^5$, $A_2 = 3.23 \cdot 10^3$,
 619 $R_1 = 4.15$, $R_2 = 0.95$, $\bar{\rho} = 1.63 \cdot 10^{-3}$ and $\gamma = 1.3$. On the right of the interface,
 620 the water is described through the stiffened EOS with $\gamma = 7.15$ and $p_s = 3.309 \cdot 10^2$.
 621 Initial data for this test problem is:

$$622 \quad (\rho_0, u_0, p_0) = \begin{cases} (1.63 \cdot 10^{-3}, 0.0, 8.381 \cdot 10^3), & 0 \leq x < 0.16, \\ (1.025 \cdot 10^{-3}, 0.0, 1.0), & 0.16 < x \leq 3. \end{cases}$$

623 The results are shown in Fig.7. Clearly, both first and second-order RD schemes
 624 capture the interfaces very accurately, while second-order scheme is more accurate in
 625 the regions of smooth flow.

626 **9. Conclusions.** In this paper we have proposed a Residual Distribution (RD)
 627 scheme for the Lagrangian hydrodynamics based on the staggered finite element for-
 628 mulation of [15]. We have developed an efficient mass matrix diagonalization algo-
 629 rithm which relies on the modification of the time-stepping scheme and gives rise to
 630 an explicit high order accurate scheme. Moreover, the scheme is parameter-free and
 631 doesn't require any artificial viscosity. The one-dimensional numerical tests consid-
 632 ered in this paper show the robustness of the method for problems involving very
 633 strong shock waves. Further research includes the extension of the present method to


 FIG. 4. *Solution of the strong shock problem at $T = 0.012$*

634 multiple dimensions and higher order in space and time.

635 **Acknowledgments.** We thank Dr. A. Barlow from AWE, UK, for introducing
 636 us to this problem. We have had several very interesting conversations on this topic,
 637 and the selection of numerical examples has also been influenced by these discus-
 638 sion. The authors thanks the financial support of the Swiss SNF via the grant #
 639 200021_153604 ("High fidelity simulation for compressible material"). R.A. has been
 640 partially supported by this grant and S.T. has been fully supported by this grant.

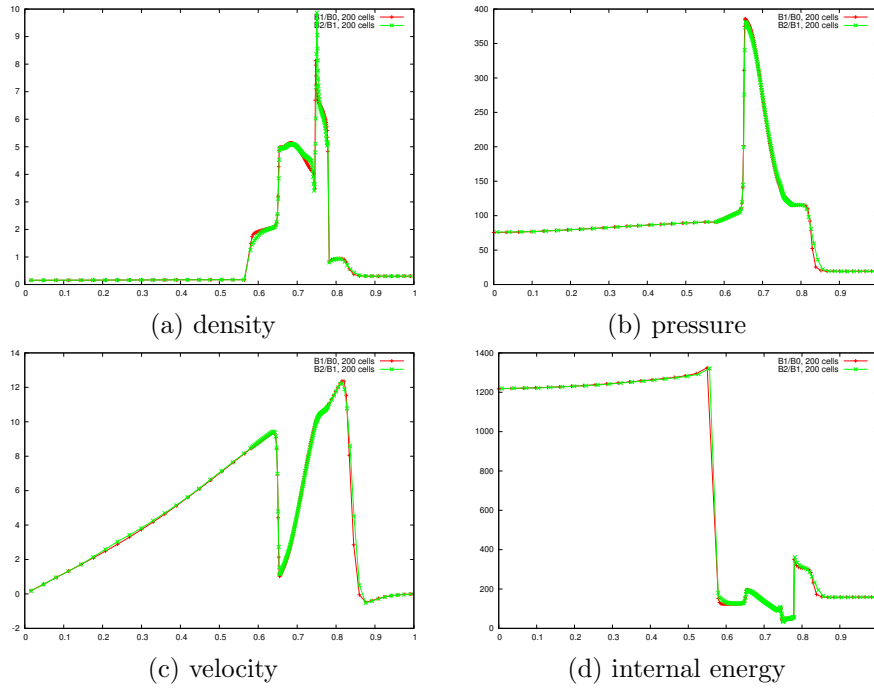


FIG. 5. Solution of the Woodward-Colella blast wave interaction problem at $T = 0.038$

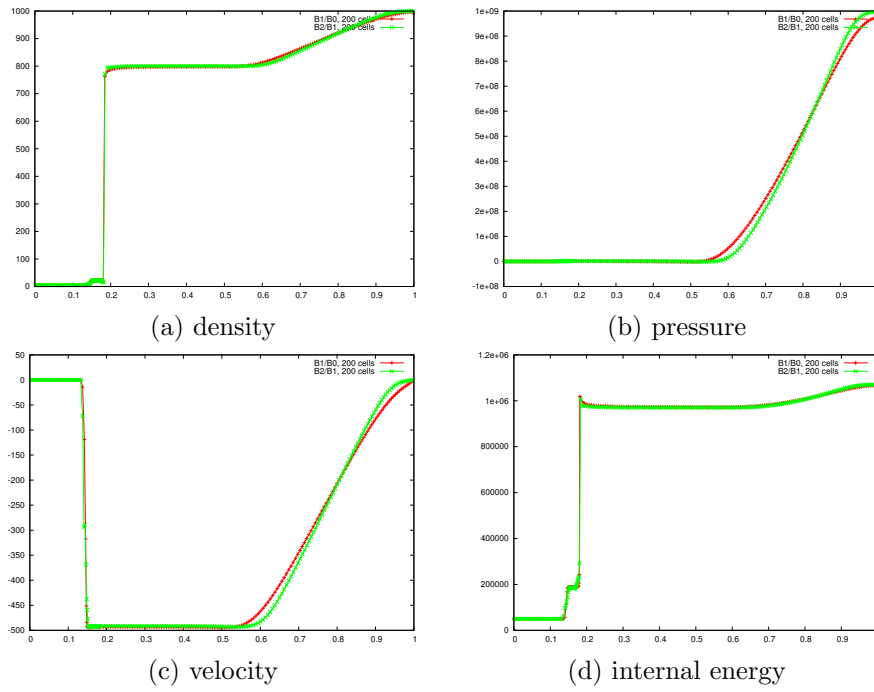


FIG. 6. Solution of the gas-liquid shock tube problem at $T = 0.00024$

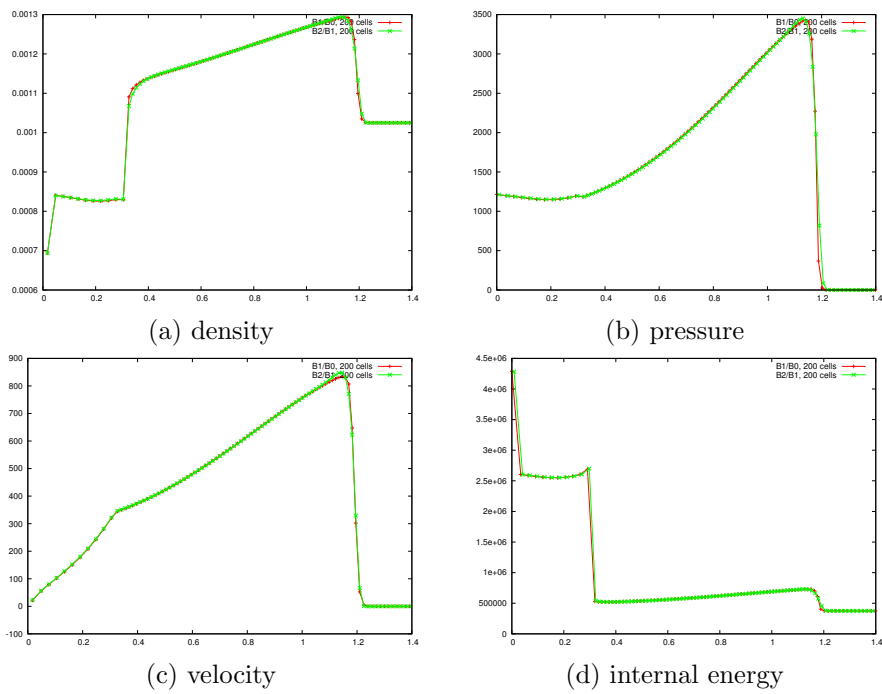


FIG. 7. Solution of the underwater TNT explosion problem at $T = 0.00025$

REFERENCES

641

- 642 [1] R. ABGRALL, *On a class of high order schemes for hyperbolic problems*, in Proceedings of the
643 International Congress of Mathematicians, S. Y. Jang, Y. R. Kim, D.-W. Lee, and I. Yie,
644 eds., vol. IV, 2014, pp. 699–726. ISBN 978-89-6105-807-0.
- 645 [2] R. ABGRALL, P. BACIGALUPPI, AND S. TOKAREVA, *How to avoid mass matrix for linear hyper-*
646 *boldic problems*, in Proceeding of ENUMATH 2015, vol. Lecture Notes in Computational
647 Science and Engineering, Springer, 2016.
- 648 [3] R. ABGRALL, A. LARAT, AND M. RICCHIUTO, *Construction of very high order residual distribu-*
649 *tion schemes for steady inviscid flow problems on hybrid unstructured meshes*, J. Comput.
650 Phys., 230 (2011).
- 651 [4] R. ABGRALL AND P. ROE, *High order fluctuation schemes on triangular meshes*, J. Sci. Com-
652 put., 19 (2003), pp. 3–36.
- 653 [5] A. BARLOW, *A compatible finite element multi-material ALE hydrodynamics algorithm*, Inter-
654 nat. J. Numer. Methods Fluids, 56 (2007), pp. 953–964.
- 655 [6] W. BOSCHERI, D. BALSARA, AND M. DUMBSER, *Lagrangian ADER-WENO finite volume*
656 *schemes on unstructured triangular meshes based on genuinely multidimensional HLL Rie-*
657 *mann solvers*, J. Comput. Phys., 267 (2014), pp. 112–138.
- 658 [7] W. BOSCHERI AND M. DUMBSER, *Arbitrary-Lagrangian-Eulerian one-step WENO finite volume*
659 *schemes on unstructured triangular meshes*, Comm. Comp. Phys., 14 (2013), pp. 1174–
660 1206.
- 661 [8] W. BOSCHERI AND M. DUMBSER, *A direct Arbitrary-Lagrangian-Eulerian ADER-WENO finite*
662 *volume scheme on unstructured tetrahedral meshes for conservative and non-conservative*
663 *hyperbolic systems in 3D*, J. Comput. Phys., 275 (2014), pp. 484–523.
- 664 [9] W. BOSCHERI, M. DUMBSER, AND O. ZANOTTI, *High order cell-centered Lagrangian-type finite*
665 *volume schemes with time-accurate local time stepping on unstructured triangular meshes*,
666 J. Comput. Phys., 291 (2015), pp. 120–150.
- 667 [10] W. BOSCHERI, R. LOUBÈRE, AND M. DUMBSER, *Direct Arbitrary-Lagrangian-Eulerian ADER-*
668 *MOOD finite volume schemes for multidimensional hyperbolic conservation laws*, J. Com-
669 put. Phys., 292 (2015), pp. 56–87.
- 670 [11] E. BURMAN AND P. HANSBO, *Edge stabilization for Galerkin approximation of convection-*
671 *diffusion-reaction problems*, Comput. Methods Appl. Mech. Engrg., 193 (2004), pp. 1437–
672 1453.
- 673 [12] E. J. CATAMANA, D. E. BURTON, AND M. J. SHASHKOV, *The construction of compatible hydro-*
674 *dynamics algorithms utilizing conservation of total energy*, J. Comput. Phys., 146 (1998),
675 pp. 227–262.
- 676 [13] J. CHENG AND C.-W. SHU, *A high order eno conservative Lagrangian type scheme for the*
677 *compressible Euler equations*, J. Comput. Phys., 227 (2007), pp. 1567–1596.
- 678 [14] J. CHENG AND C.-W. SHU, *Positivity-preserving Lagrangian scheme for multi-material com-*
679 *pressible flow*, J. Comput. Phys., 257 (2014), pp. 143–168.
- 680 [15] V. DOBREV, T. KOLEV, AND R. RIEBEN, *High order curvilinear finite element methods for*
681 *Lagrangian hydrodynamics*, SIAM J. Sci. Comput, 34 (2012), pp. B606–B641.
- 682 [16] M. DUMBSER, *Arbitrary-Lagrangian-Eulerian ADER-WENO finite volume schemes with time-*
683 *accurate local time stepping for hyperbolic conservation laws*, Comp. Meth. Appl. Mech.
684 Eng., 280 (2014), pp. 57–83.
- 685 [17] M. DUMBSER AND W. BOSCHERI, *High-order unstructured Lagrangian one-step WENO finite*
686 *volume schemes for non-conservative hyperbolic systems: Applications to compressible*
687 *multi-phase flows*, Computers & Fluids, 86 (2013), pp. 405–432.
- 688 [18] C. FARHAT, J.-F. GERBEAU, AND A. RALLU, *Fiver: a finite volume method based on exact*
689 *two-phase Riemann problems and sparse grids for multi-material flows with large density*
690 *jumps*, J. Comput. Phys., 231 (2012), pp. 6360–6379.
- 691 [19] G. GEORGES, J. BREIL, AND P.-H. MAIRE, *A 3D GCL compatible cell-centered Lagrangian*
692 *scheme for solving gas dynamics equations*, J. Comput. Phys., 305 (2016), pp. 921–941.
- 693 [20] P.-H. MAIRE, R. ABGRALL, J. BRIL, AND J. OVADIA, *A cell-centered Lagrangian scheme for*
694 *two-dimensionnal compressible flow problems*, SIAM J. Sci. Comput., 29 (2007), pp. 1781–
695 1824.
- 696 [21] M. RICCHIUTO AND R. ABGRALL, *Explicit runge-kutta residual-distribution schemes for time*
697 *dependent problems*, J. Comput. Phys., 229 (2010), pp. 5653–5691.
- 698 [22] G. SCOVAZZI, M. CHRISTON, T. HUGHES, AND J. SHADID, *Stabilized shock hydrodynamics: I*
699 *A Lagrangian method*, Comput. Methods Appl. Mech., 196 (2007), pp. 923–966.
- 700 [23] M. SHASHKOV, P. MAIRE, RIEBEN, AND A. BARLOW, *Review of Lagrangian methods*, J. Comput.
701 Phys., (2016).

- 702 [24] E. F. TORO, *Riemann Solvers and Numerical Methods for Fluid Dynamics*, Springer-Verlag,
703 2009.
- 704 [25] F. VILAR, P.-H. MAIRE, AND R. ABGRALL, *A discontinuous galerkin discretization for solving*
705 *the two-dimensional gas dynamics equations written under total Lagrangian formulation*
706 *on general unstructured grids*, J. Comput. Phys., 276 (2014), pp. 188–234.
- 707 [26] F. VILAR, C. SHU, AND P.-H. MAIRE, *Positivity-preserving cell-centered Lagrangian schemes*
708 *for multi-material compressible flows: From first-order to high-orders. part i: The one-*
709 *dimensional case*, J. Comput. Phys., 312 (2016), pp. 385–415.
- 710 [27] F. VILAR, C. SHU, AND P.-H. MAIRE, *Positivity-preserving cell-centered Lagrangian schemes*
711 *for multi-material compressible flows: From first-order to high-orders., part ii: The two-*
712 *dimensional case*, J. Comput. Phys., 312 (2016), pp. 416–442.
- 713 [28] J. VON NEUMANN AND R. D. RICHTMYER, *A method for the numerical calculation of hydrody-*
714 *namics shocks*, J. Appl. Phys., 21 (1950), pp. 232–237.
- 715 [29] M. L. WILKINS, *Methods in Computational Physics*, vol. 3, Academic Press, New York, 1964.
- 716 [30] P. WOODWARD AND P. COLELLA, *The numerical simulation of two-dimensional fluid flow with*
717 *strong shocks*, J. Comput. Phys., 54 (1984), pp. 115–173.